Journal of Traditional and Complementary Medicine 7 (2017) 178–187

Contents lists available at ScienceDirect

Journal of Traditional and Complementary Medicine

journal homepage: http://www.elsevier.com/locate/jtcme

Original article

Boiling-induced nanoparticles and their constitutive proteins from *Isatis indigotica* Fort. root decoction: Purification and identification

Jianwu Zhou, Jie Liu, Dai Lin, Guanzhen Gao, Huiqin Wang, Jingke Guo, Pingfan Rao, Lijing Ke*

SIBS, CAS-ZJGSU Joint Centre for Food and Nutrition Research, Zhejiang Gongshang University, Hangzhou 310012, China

ARTICLE INFO

Article history:
Received 6 April 2016
Received in revised form
27 June 2016
Accepted 15 August 2016
Available online 20 October 2016

Keywords:
Nanoparticles
Boiling-induced assembly
Glycated protein
Herbal decoction
Colloidal aggregates
Chromatographic purification

ABSTRACT

Colloidal particles are essential components of sun-dried *Isatis indigotica* Fort. roots (Ban-Lan-Gen in Chinese, BLG) decoction. Nanoparticles (NPs) were isolated from BLG decoction with size exclusion chromatography and characterized. Their average diameter is ~120 nm, reversibly responding to pH and temperature changes. They promoted the growth of normal cells but suppressed that of cancerogenic cells and macrophages. Two constitutive glycated proteins were identified from the NPs, namely BLGP1 and BLGP2. Their N-terminal amino acid sequences were V-X-R-E-V-V-K-D-I and V-V-R-E-V-V-K-D-I-A-G-A-V-Q-T-N-E-Q-Y. Their full-length cDNA sequences were cloned to obtain the highly homological amino acid sequences of non-glycated proteins, whose theoretical molecular weights are 21831.64 Da and 21841.67 Da. Using pepsin hydrolysis and mass spectrometry, four possible glycation adducts were identified in BLGP1, whereas one in BLGP2. To conclude, bioactive nanoparticles isolated from the herbal decoction are intelligent nanoassemblies composed of a new boiling-stable protein. Glycation plays a critical role in heat-induced formation of these nanoassemblies. The novel, intelligent, safe and stable nano-carriers for drug delivery may be developed using BLG NPs as prototype.

1. Introduction

Like many other Chinese herbs, *Isatis indigotica* Fort. (Chinese woad) is a biennial herbaceous plant species planted widely in China with a few hundred years of medicinal use. To date, the sun-dried roots of *I. indigotica* (Radix Isatidis, Ban-Lan-Gen) and their extracts are popularly used alone or in combination with other herbs to treat a wide variety of infectious and inflammatory diseases, such as influenza, herpes, acute hepatitis, arthritis and encephalitis B.[1–3] Like many other Chinese herbal medicine, decoction is its major administration formula. The granules of Radix Isatidis are also widely used, which is basically the dried powder of its decoction.[4] The decoction can inhibit viral infection via protection of host cells rather than killing virus,[5] increase the spleen weight and number of lymphocytes and antagonize the immunosuppressive actions of hydrocortisone.[6] One of the most notable chemical changes occurred during preparation of Ban-Lan-Gen decoction is the significant reduction in the content of free basic amino acids, i.e. arginine and lysine, and reducing sugars, i.e. glucose, after sun-drying and boiling. The Maillard reaction occurred is the driven force of the above chemical evolution and produces a high content of non-enzymatic glycated proteins[7] with elevated structure stability and solubility at higher temperature,[8,9] e.g. in decocting process. Besides, Ban-Lan-Gen decoction contains a great number of colloidal particles and aggregates.

Boiling extraction (decocting) is the earliest and most popular way of preparing herbal decoction. The intensive boiling process migration a great number of compounds from plant materials to the soup, interaction among extracted coexisting actives and the formation of a multiple-phase dispersion. As reported in a previous study, colloids-like aggregates were observed in all the decoctions of 60 medicinal herbs and 24 Chinese herbal formulae, and were able to survive in the gastro-intestinal environment, pass through the Caco-2 cell monolayer and correlated to the activities of decoction.[10] Aggregates even as the precipitates from a two-herb decoction, containing *Aconitum carmichaelii* Debx. (Fu-Zi) and *Radix Rhizoma Glycyrrhizae* (licorice, Gan-Cao), increased the mean

* Corresponding author. Room 407, No. 1 Laboratory Bld., No. 149 Jiaogong Road, Hangzhou 310012, China. Fax: +86 571 8805 6656.
E-mail address: lijingke@zjgsu.edu.cn (L. Ke).

Peer review under responsibility of The Center for Food and Biomolecules, National Taiwan University.

http://dx.doi.org/10.1016/j.jtcme.2016.08.007

residence time and absorbed doses of diester diterpenoid alkaloids in gastrointestinal tract and blood after oral administration.[11] On the other hand, the synergic effects between various herbal ingredients and compositions of TCM decoction have been proven by studies *in vitro* and *in vivo*,[12,13] despite the general mechanism of which has not yet been elucidated.[14] Therefore, in respect to the individual active compositions, the aggregates facilitated by noncovalent bonding among multiple molecules may provide an infrastructure for active compositions to conduct their synergic curative effects. Among these aggregates and precipitates, colloidal particles may be the dominant participates, as they are self-assembled by the extracted compounds carrying principle bioactive phytochemicals, i.g. ephedrine embedded colloidal nanoparticles in Ma-Xing-Shi-Gan decoction are expected to cause much less safety concerns[15] and displayed similar biological function with the decoction itself.[16] Wang et al. reported the cluster size of compositions from water decoction of *Pueraria lobata* var. *thomsonii* Benth (radix, Feng-Ge) is correlated to the amount of herb used and is relevant to the oral drug absorption efficiency and the reduction of the octapeptide angiotensin II.[17] Colloids in TCM decoction is merely the sole case of particulates which integrate various active compounds and therefore change their properties and biological functions. For instance, milk protein forms aggregates with chocolate flavonoids and coffee polyphenols and caused the reduction in both bioavailability and health benefits.[18,19] The opposite effects of molecular assembly or aggregates occurred in the above complex system of natural products indicates the composition, bioactivity and structural characteristics of these colloids ought to be studied to understand their role in the healing decoction.

Recently, protein nanoparticles have drawn rising attention in the field of nanotechnology. A range of plant-source proteins have been used to fabricate colloidal delivery systems, including zein, whey proteins, soy proteins, caseinate and boiling stable proteins (hydrophilins).[20] Many of these proteins are GRAS (generally recognized as safe) food ingredients.[21] Taking whey proteins as an example, comprehension of the aggregation mechanism of these proteins is warranted for manipulating the properties of proteins colloids and facilitating the possible applications in food and pharmaceutical industry. The changes of protein structures were observed prior to protein aggregation, which include partial unfolding of the tertiary structure and conformational changes of secondary structure. As a consequence, hydrophobic sites or free −SH groups are exposed to molecular surface, therefore enhance intermolecular interaction led to the formation of soluble aggregates.[22,23] The triggers of protein aggregation, including heating[24] and protein glycation,[25] were extensively investigated while the latter has been considered as a promising approach for protein modification.[26] It can alter the hydrophobicity and the secondary structure of the protein, improve the thermo-stability and facilitate protein aggregations.[27]

In this study, the colloidal nanoparticles (NPs) were isolated from Ban-Lan-Gen boiling water extracts, whose constitutive proteins were characterized with SDS-PAGE. To get further insights on the assembly mechanisms of NPs from Ban-Lan-Gen decoction, which may be induced upon glycation and boiling, the characterization of these NPs and structural characterization of their component proteins were performed.

2. Material and methods

2.1. Raw materials, chemicals and cell lines

The sun-dried roots (Ban-Lan-Gen, BLG) and fresh roots of *I. indigotica* Fort. were collected from the same GAP (Good Agricultural Practice) field in Fuyang (Anhui Province, China). All the chemicals used in this study were of reagent/analytical grade from Sinopharm Chemical Reagent Co., Ltd (Shanghai, P. R. China). Protein Molecular Weight Marker (Beyotime Biotechnology), MTT (Sigma–Aldrich). Human normal hepatocytes (L-02), human hepatoblastoma cells (Hep-G2), rat alveolar macrophage cells (NR8383) and human cervical carcinoma cells (HeLa-229) were purchased from the Type Culture Collection of Chinese Academy of Science (Shanghai, China).

2.2. BLG decoction preparation

To prepare the BLG decoction, sliced BLG were soaked in distilled water (1:8, w/v) for 30 min at room temperature with stirring, then boiled for 60 min, cooled to room temperature and filtered through two layers of cotton gauze.

2.3. Separation of nanoparticles from BLG decoction

The nanoparticles from BLG decoction were separated with a size-exclusion gel chromatography with multi-angle laser light scattering (SEC-MALLS) as described in Ref. 15. The fraction with strong signals at both light scattering and UV280 nm were collected and pooled for further analysis.

2.4. Dynamic Light Scattering measurement

Particle size measurements were performed by Dynamic Light Scattering analysis (DLS) on a Zetasizer Nano device (Malvern Instruments, Worcestershire, UK). Sample aqueous suspension (1 mL) was centrifuged at 400 g for 10 min (Model CF16RXII, Hitachi Koki Co., Ltd., Japan). The supernatant, without dilution, was moved to the disposable 10 mm cuvettes for measurement at 25 °C. Deionized water or chromatograph elution buffer was used as background control.

2.5. Scanning electron microscopy (SEM)

Scanning electron microscopy (SEM) was performed with a Cold Field Emission S-4800 Scanning Electron Microscope (Hitachi, Tokyo, Japan) operated under an acceleration voltage of 5 kV. The particles were collected with 0.22 μm cellulose acetate membrane and coated with gold with sputter coater (E-1010, Hitachi Instruments, Japan) to render them electrically conductive. The images were taken with 15 k magnification and 500 nm scale bar.

2.6. Denatured gel electrophoresis and periodic acid–Schiff (PAS) staining

Gel electrophoresis (SDS–PAGE) was performed under reducing conditions on a 0.1% SDS–12% polyacrylamide slab-gel according to Laemmli method.[28] PAS staining was performed as below: gel was fixed with 10% trichloroacetic acid for 60 min, washed twice with deionized (DI) water for 1 min, oxidized with 1% periodic acid for 60 min, washed twice with DI water for 15 min, stained with Schiff reagent for 60 min, washed with DI water for 1 min, added 0.25% sodium metabisulphite–3.5% acetic acid solution for overnight at 4 °C and finally washed with DI water again.

2.7. Separation of constituent proteins from BLG aqueous extract

The ground BLG (100 g) was extracted with 300 mL of PBS buffer (0.01 M, pH 7.2, 0.1 M NaCl) overnight at 4 °C. The extract was centrifuged at 12,000 g for 15 min (Model CF16RX, Hitachi Koki Co., Ltd., Japan) and removed debris.

The extract was diluted 2 times with 0.02 M citrate buffer (pH 3.0), loaded to a pre-equilibrated SP-650M cationic exchange column (3.9 × 300 mm, 65 μm, Tosoh Biosep, Montgomeryville, PA) and eluted with a linear gradient (0 M–0.2 M in 135 min, 0.5 M–1.0 M in 185 min) of sodium chloride in citrate buffer (0.02 M, pH 3.0) at 2.0 ml/min, monitoring at 280 nm.

The fraction containing NPs constituent proteins were pooled for further purification with a POROS® HP2 hydrophobic interaction chromatography column (4.6 × 250 mm, PerSeptive Biosystems, Framingham, MA). The column was pre-equilibrated with 0.02 M phosphate buffer containing 1.5 M $(NH_4)_2SO_4$, SP-650M fraction (50 mL) was adjusted to the same $(NH_4)_2SO_4$ concentration and loaded at 1 ml/min. The proteins with molecular weight 22.5 kDa and 25.1 kDa were eluted and collected with a linear gradient from 1.2 to 0.6 M of $(NH_4)_2SO_4$ in 120 min, monitored at 280 nm. The two protein fractions were freeze-dried for further analysis.

2.8. Protein N-terminal sequencing

Automated Edman degradation was performed using an Applied Biosystems 491 Procise sequencer. The resultant amino acid derivative (a phenylthiohydantoin amino acid) was analyzed with a capillary liquid chromatography system. The primary structure was obtained by comparing the elution position of standard PTH-AA. The limit of detection of phenylthiohydantoin (PTH)-amino acids was 0.5 Pm8.

2.9. Amplification (RACE) and cloning of full-length cDNAs

Five hundred milligrams fresh root of *I. indigotica* Fort was ground into fine powder in an RNase-free grinder using liquid nitrogen. Polyadenylated mRNA isolation was performed using an mRNA isolation kit (Dynal Biotec., UK). The first strand of 5′- and 3′-RACE cDNA was synthesized using a Smart™ RACE cDNA amplification kit (Clontech, UK).

The degenerate primer (primer 1, 5′-ARGAYATHGCN GGNGCNGTNCARACNAA-3′) for 3′-RACE was complementary to amino acid sequences of obtained BLG proteins by N-terminal sequencing. The 3′-RACE reactions employed a NUP primer (supplied with the kit) and primer 1. The 3′-RACE products were purified using a Wizard SV Gel and PCR Clean-up System (Promega, US), cloned using a pGEM-T vector system (Promega Corporation) and sequenced using an ABI 3100 automated capillary DNA sequencer.

From the cDNA sequences obtained, a gene-specific antisense primer (antisense primer 2, 5′-CGGTTCCAATGATTCCGTCAAAGATG-3′) for the 5′-RACE reaction was designed to a region that is highly conserved in all the obtained cDNA sequences. The 5′-RACE reactions were performed by using a NUP primer and an antisense primer. Generated products were purified, cloned and sequenced as described above.

2.10. Determination of glycation adducts

The locations and structures of glycation adducts within glycated BLG proteins were determined, using a modified method[29] as summarized in the diagram below. Briefly, the BLG proteins dissolved in KCl–HCl buffer (0.1 M, pH 2.5, 1 mg/ml) were digested at 37 °C for 2 h with pepsin (EC3.4.23.1; 3300 U per mg) at an approximately physiological ratio of enzyme/substrate (1:20 wt:wt), fractionated with reversed-phase HPLC (Jupiter C18 column, 250 mm × 4.6 mm, 5 μm, Phenomenex, UK) and analyzed by a Thermo LCQ™ 'classic' electrospray ion-trap mass spectrometer (Finnigan MAT, California, USA). The LC-MS system, data acquisition and processing were managed by Xcalibur software, (1.2 version; Thermo Fisher Scientific). The assignment of observed ions to the corresponding amino acid sequences was based on the known sequence translated from full-length cDNA and TrEMBL, and the tools Peptide Mass and FindPept available at www.expasy.org.

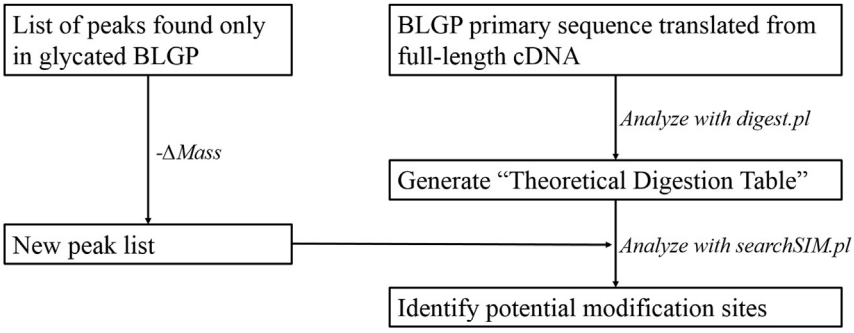

2.11. Cell culture and MTT assay

Human normal hepatocytes (L-02), human hepatoblastoma (Hep-G2) cells, rat alveolar macrophage (NR8383) cells and human cervical carcinoma (HeLa-229) cells were used to evaluate the influence of BLG NPs on the cellular viabilities and proliferation, with MTT assay. Samples were adjusted to the universal serial protein concentrations (2.20, 1.10, 0.55, 0.28, 0.14, 0.07 mg/mL), added to the cells in 96-well plates, 4 duplicates each, and cultured at 37 °C, 5% CO_2 for 48 h. The cell proliferation rate was calculated with the equation below (Means ± SD, n = 4): Proliferation Rate = (O.D.570nm_sample − O.D.570nm_control)/O.D.570nm_control × 100%. The significant levels were examined with Student's t-test and ranked as $P < 0.05$ or $P < 0.01$.

3. Results

3.1. Separation of nanoparticles from BLG soups

The size exclusion chromatography in couple with multi-angle laser light scattering (SEC-MALLS) has been used to separate and characterize a wide range of synthesized nanoparticles from their reaction mixtures.[30,31] Our recent work demonstrated this approach could separate the colloidal nanoparticles even from a much more complex chemical cocktail, the herbal boiling aqueous extracts named Ma-Xing-Shi-Gan-Tang decoction.[15]

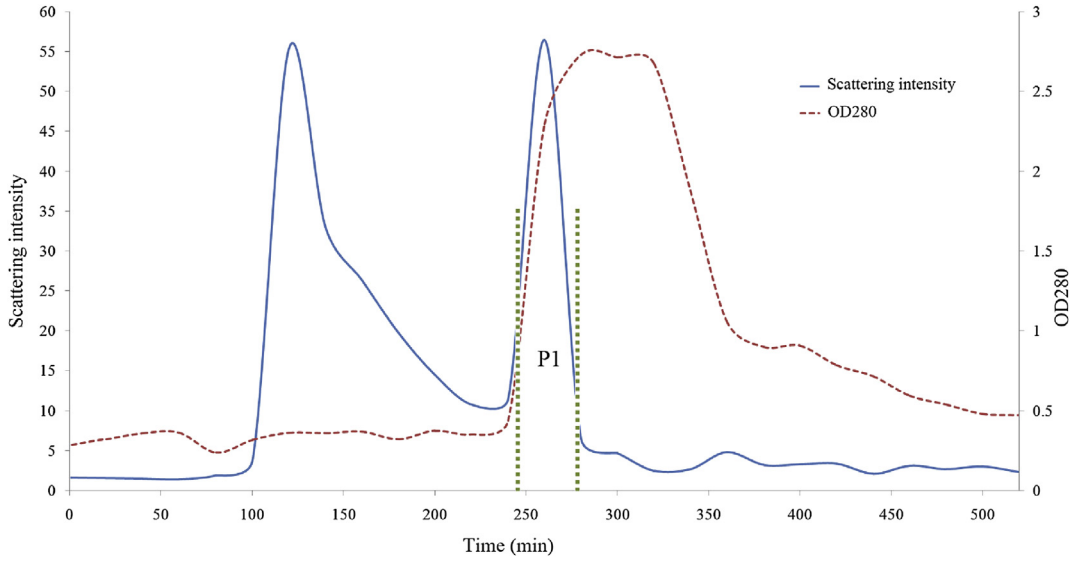

Fig. 1. BLG decoction was fractionated by a Sephacryl S-1000 column (1.0 cm × 100 cm) equilibrated with 0.02 M Citrate buffer (pH 5.0). The column was eluted with the same buffer at a flow rate of 0.34 mL/min. The red dash curve shows the elution profile of BLG decoction at 280 nm, while the blue solid curve shows the light scattering intensities at 90° of fractions by multi-angle laser light scattering. The green dotted line area refers to the fraction named P1, which was collected and pooled for further investigation.

As is shown in Fig. 1, two major finely separated peaks of light scattering were observed in chromatogram of SEC-MALLS. The strong light scattering intensity could distinguish the particles from other high molar mass single molecules in UV chromatogram. The calculation of MALLS indicates the average size of particles or particle clusters within the first light scattering peak are over 1000 nm. The second fraction with both intense light scattering signals and high UV absorption at 280 nm contains smaller particles (showed as P1 in Fig. 1), which implies the possible participation of protein in the particle assembly. Fraction P1 was collected and pooled for further investigation. Among the neighboring fractions to P1, the average particles size was 162 nm and 98 nm, respectively, which is close to the size of P1 (122 nm) and exhibits a fine time-resolved particle size resolution of the chromatographic separation.

3.2. Characterization of the separated colloidal nanoparticles

The particle size distribution of P1 fraction was showed in Fig. 2, which indicated an average diameter of 122 nm, measured with a Zetasizer Nano light scattering device. P1 nanoparticles were pH and temperature responsive. As shown in Fig. 3A, the average size was smallest as 117 nm at pH 5, which was doubled or even tripled by adjusting pH to basic (pH8-10) or acidic (pH2-3) conditions. When adjusted back to pH6, the higher order aggregates dispersed and particle size was restored (~120 nm). On the contrary, rising temperature caused the significant decline in average size, i.e. 82 nm at 100 °C (as shown in Fig. 3B). The particle sized up again when the suspension was cooled down to room temperature (20 °C). The temperature- or pH-induced nanoparticle size change was reversible. As shown in Fig. 4, P1 NPs remained in the same size within 48 h at room temperature (20 °C) and formed no visible sediments after 5 d storage, indicating a good stability in aqueous suspension.

The SEM morphologic observation revealed the separated NPs are spherical with diameters ranged from a few dozen to a few hundred nanometers (as shown in Fig. 5). The main particle population was consistent with the size distribution range determined by light scattering method (max. 200 nm, Fig. 2), while some particles were bigger than 200 nm. It may be attributed to the secondary aggregation occurred during the sample preparation of SEM.

The bioactivity of P1 NPs was subsequently investigated as impacts on cytoviabilities of four cultured cell lines, with different organ origins, including human hepatoblastoma (Hep-G2) cells, human cervical carcinoma (HeLa-229) cells, human normal

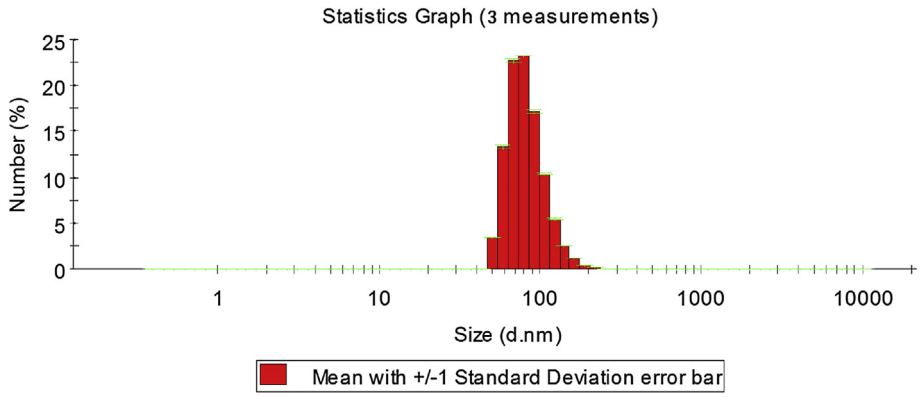

Fig. 2. The particle size distribution of P1 particles measured by a Zetasizer Nano device laser light scattering.

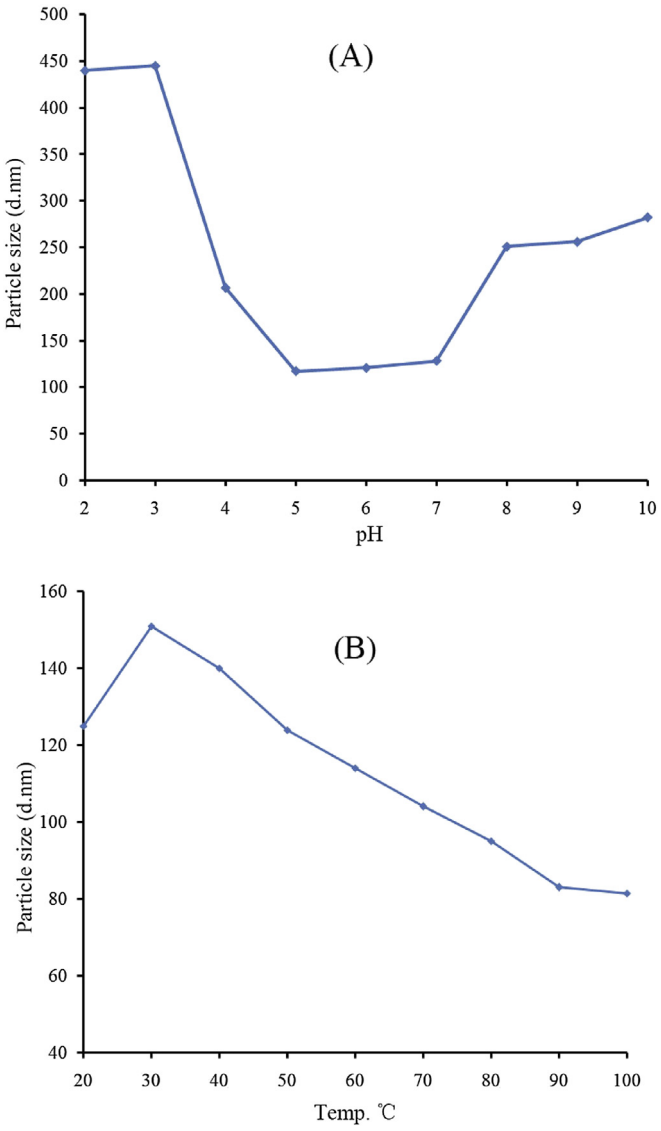

Fig. 3. P1 NPs showed their pH and temperature sensitive nature. (A) Mean size of NPs corresponding to pH; (B) Mean size of NPs corresponding to temperature.

hepatocytes (L-02) and rat alveolar macrophage (NR8383) cells, as is showed in Fig. 6. The NPs displayed slight or moderate cytotoxicity in all cell lines tested.[32] The NPs increased the growth of L-02 by about 154% (as was compared to blank control), while significantly suppressed the proliferation of NR8383 by about 40% at the concentration of 0.14 mg/ml. At the meanwhile, the NPs mildly increased the proliferation of Hep-G2 and HeLa cells at relatively low concentrations, but suppressed it at concentrations higher than 1.1 mg/ml. Interestingly, 48 h exposure of P1 NPs did not suppress the cyto-viability of any cell type tested for more than 50% at dosage as high as 2.2 mg/mL, while many artificially manufactured nanoparticles with inorganic materials exhibit much higher cytotoxicity (IC50 < 0.1 mg/mL) upon pulmonary epithelial and macrophage cells after a shorter (24 h) exposure.[33] Although NR8383 macrophages seemed more vulnerable to P1 NPs induced cytotoxicity, the suppression was rather moderate since NPs at high dose did no more harm than the low dose.

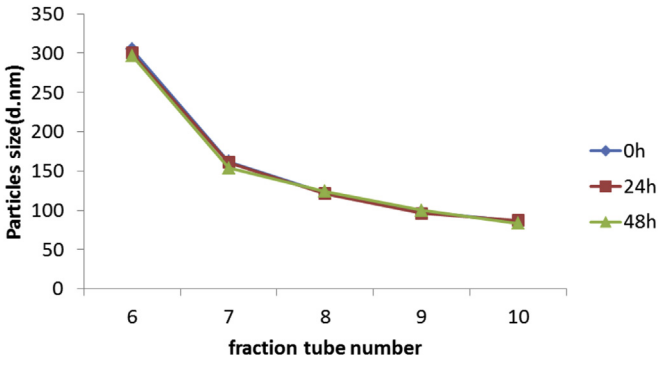

Fig. 4. NPs separated with size exclusion chromatography were stable within 48 h at 20 °C.

3.3. Determination of constitutive proteins within P1 NPs by SDS-PAGE

PAGE and SDS-PAGE were performed to analyze proteins within P1 NPs fraction. Two protein bands with MW 25.1 kDa and MW 22.5 kDa were shown on SDS-PAGE gel (Fig. 7, lane 1), named as BLGP1 and BLGP2, respectively. The subsequent PAS staining revealed both of them are glycated proteins (Fig. 7, lane 4). In comparison, no protein band was observed on PAGE gel, indicating that the proteins are incorporated in complex like NPs, rather than staying alone, via non-covalent bonds which can be de-associated by the strong anionic strength of SDS.[34]

3.4. Purification and characterization of component proteins

Two proteins of 25.1 kDa (BLGP1) and 22.5 kDa (BLGP2) were purified. As shown in Fig. 8, the fractions contained BLGP1 and BLGP2 were finely separated, marked as P1 and P2 in the HP2 chromatogram. SDS-PAGE image (shown in Fig. 7 lane 2 and 3) and PAS staining (Fig. 7 lane 5 and 6) prove they are target glycated protein. The isoelectric points (pI) of BLGP1 and BLGP2 were 6.68 and 6.58, respectively. The N-terminal amino acid sequences of purified proteins were determined as V-X-R-E-V-V-K-D-I and V-V-R-E-V-V-K-D-I-A-G-A-V-Q-T-N-E-Q-Y by Edman degradation (X refers to uncertain amino acid).

For obtaining their full-length cDNA, 3′-RACE was performed by using a gene specific prime (5′-ARGAYATHGCNGGNGCNGTNCAR-ACNAA-3′), which was complementary to amino acid sequences of obtained BLG proteins by N-terminal sequencing. From the cDNA sequences obtained from 3′-RACE, a gene-specific antisense primer (antisense primer 2, 5′- CGGTTCCAATGATTCCGTCAAAGATG-3′) for the 5′-RACE reaction was designed to a region that is highly conserved in all the obtained cDNA sequences.

Finally, two full-length cDNAs were consistently cloned from *I. indigotica* Fort. fresh root cDNA library (GenBank: ACV83939.1 and ACV83940.1). These two full-length cDNAs show very high structural homology, both of the open-reading frames consist of 226 amino acid residues, beginning with a putative signal peptide of 23 amino acid residues and followed by a spacer peptide -KQ- and a mature protein region downstream of the signal peptide (Fig. 9A and B). The amino acid sequences of non-glycated BLG proteins were obtained according to their full-length cDNAs. The calculated theoretical M_w of non-glycated BLGP1 and BLGP2 are 21831.64 and 21841.67 Da, respectively. The significant differences between the measured values (25.1 and 22.5 kDa) and theoretical values (approx. 21.8 kDa) of glycated proteins molecular weights are possibly due to the reduction on electrophoretic mobility caused by glycation. BLGP1 shows high structural similarity with BLGP2, their primary structures differ by only 7 amino acid residues substitutions. Both BLG proteins show structural similarity with Kunitz-type trypsin protease inhibitor (NCBI database), supported

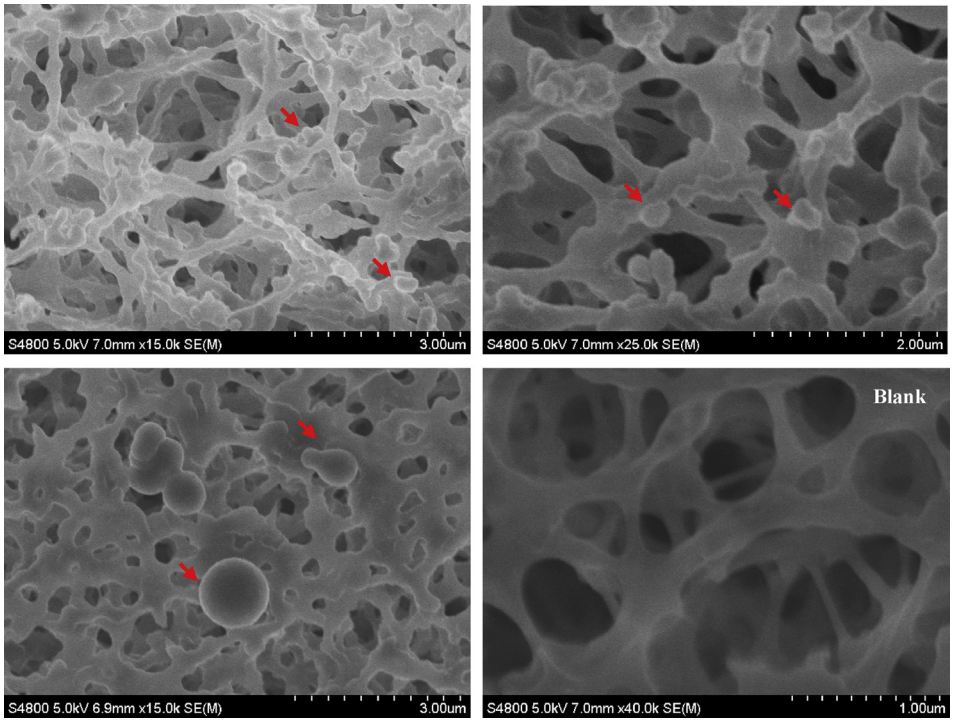

Fig. 5. SEM topographs image of BLG nanoparticles attached to the surface of a 0.45 μm cellulose acetate membrane. The image showed spherical NPs (pointed with arrows) with sizes ranged from a few dozen to a few hundred nanometers. Picture 'Blank' shows the network structure of empty cellulose acetate membrane.

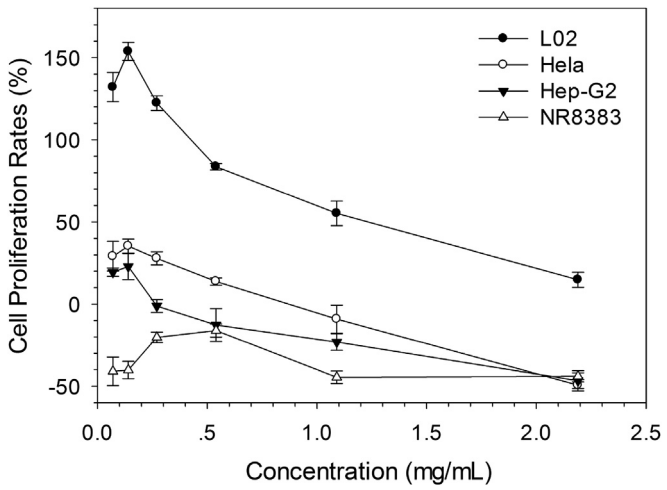

Fig. 6. Nanoparticles from BLG decoction increased or decreased the cyto-viabilities on four cultured cell lines in a dose-dependent and cell-type-dependent manner. Cell lines used shown in the figure are: human normal hepatocytes L-02 (●), human hepatoblastoma cell Hep-G2 (▼), human cervical carcinoma cell HeLa-229 (○), rat alveolar macrophage cell NR8383 (Δ). The NPs significantly promoted the growth of normal human hepatocytes while inhibited that of cancerogenic cells and alveolar macrophage ($n = 4$, $P < 0.01$).

by tests with trypsin inhibitory assay (data not shown but available on request).

According to the amino acid sequences, the BLG proteins are rich in basic amino acids, which provide possible glycated sites for Maillard reactions. For further inspecting the glycated structures of obtained BLG proteins, a method based on mass spectrometry was adopted in this study. The BLG proteins were digested with pepsin instead of trypsin, because of their trypsin inhibitory activities. The possible glycation adducts in BLG proteins were showed in Fig. 8. In BLGP1, there are four possible glycation adducts: K7—CEL/Pyr, K38—Pyr/FL-H_2O, K171—FL-$2H_2O$, R195—AFGP. In BLGP2, only one glycation adduct, R3—AFGP was detected. Higher number of glycation sites in BLGP1 may explain the 3 kDa higher molecular weight than that of BLGP2 given by SDS-PAGE, knowing glycation-induced protein structure conformation reduces the gel electrophoresis mobility rates.

4. Discussion

The naturally occurred nanoparticles or aggregates have been discovered in a range of soups, including herbal decoctions[15,16,10] and culinary soups.[35] The reason of terming these nanoparticles by "naturally occurred" is that their components are all from the natural ingredients of soups and their self-assembly is heat-induced during the boiling process. With a long history of intensive use as medicine and food, these NPs are expected to have greater potential for medicinal applications than their synthetic counterparts, arising much less safety concerns. However, the soup-derived NPs represent a much more complex colloidal system compared to other synthetic polymers and aggregates, displaying a great diversity in morphologic and chemical structures, causing difficulties in elucidating their self-assembly mechanism and structure-activity relationship.

In this study, a fraction of protein-based NPs was isolated and characterized from Ban-Lan-Gen decoction by the means of SEC-MALLS, which distinguished the protein-based NPs from others by the overlap of light scattering intensity and UV280 nm absorbance in chromatogram. The subsequent analysis of constituent protein revealed that these protein-based NPs were assembled by two glycated proteins, BLGP1 and BLGP2, between which a highly homological structure is shared. As a simplified natural occurred nano-colloids system, the protein-based NPs possessed at least two research interests: influence of NPs on the function and safety of culinary or medical decoctions, and the mechanism of heat-

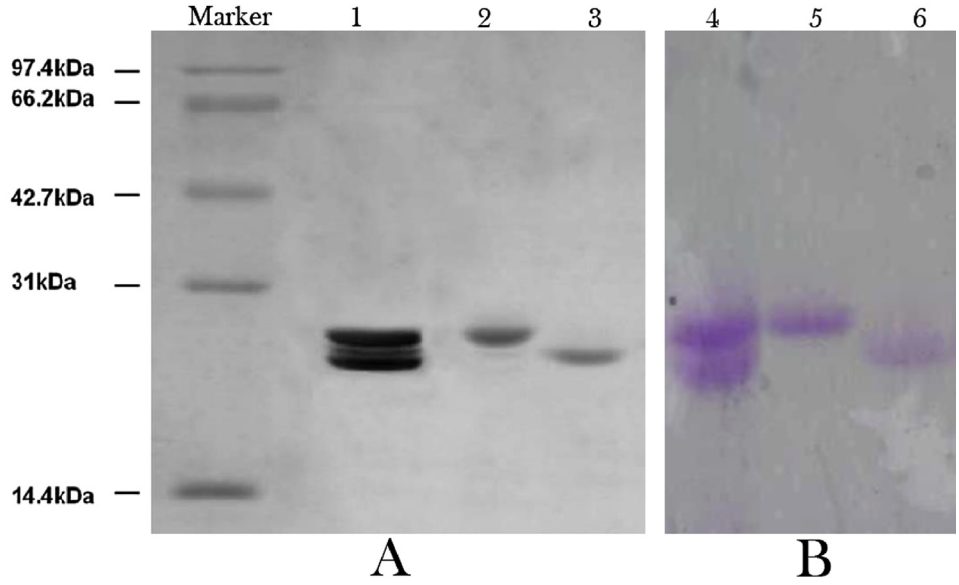

Fig. 7. SDS-PAGE of P1 NPs and purified BLG proteins. (A) Coomassie brilliant blue R-250 staining; (B) PAS staining. The samples were: MW standard proteins (Marker); SEC-MALLS isolated NPs (lane 1 & 4); HP2 chromatographic fraction P1 (lane 2 & 5); HP2 chromatographic fraction P2 (lane 3 & 6). The results indicated the NPs are composed of two major proteins (A lane 1): BLGP1 (lane 2) and BLGP2 (lane 3), both of which are glycated (lane 4, 5 & 6).

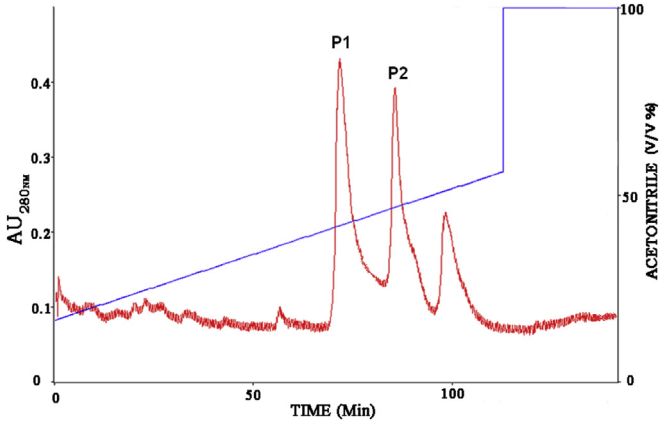

Fig. 8. BLG proteins were purified by hydrophobic interaction chromatography. The column was previously equilibrated with 0.02 M phosphate buffer containing 1.5 M $(NH_4)_2SO_4$, then eluted in a linear gradient from 1.2 M to 0.6 M of $(NH_4)_2SO_4$ in 120 min. Absorbance of the column effluent was monitored at 280 nm. In the diagram, P1 refers to fraction containing BLGP1, P2 refers to fraction containing BLGP2.

induced self-assembly. Comprehension of the above may lead to the discovery of novel proteins-based vehicles for nutrients, nutraceuticals and even pharmaceuticals.

The BLG proteins are not the mere case of plant-source proteins that self-assemble nanoparticles in the aqueous boiling extracts. The stable protein (namely SP1) from Aspen self-assembles into an oligomer of 12 identical monomers under boiling condition and remains water soluble.[36] The SP1 oligomer is ring protein complex, 11 nm in diameter, which can form large ordered arrays, and is also capable of binding gold nanoparticles (GNPs).[37] Although the 12.4 kDa protein (SP1 monomer) share significant homology with over 100 amino acid sequences from many genetically remote plant species, e.g. poplar, Arabidopsis, tomato, soybean, etc.,[36] the BLG protein share poor homology with the SP1, implying a new family of boiling stable proteins.

The isolated BLG NPs (chromatographic fraction P1) promoted the proliferation of normal cell (L-02) was strongly promoted (Fig. 6) while suppressed the carcinogenic cells and macrophages at the same concentrations (0.5–2.2 mg/ml), indicating a possible cell type-dependent selective bioactivity. Macrophages are considered as a valuable cell model to evaluate nanoparticle uptake and toxicity,[38,33] as they are the mutual immune cells in respiratory and intestinal mucosa. The vulnerability of NR8383 macrophages in this study may be attributed to the preferentially uptake of phagocytes on anionic NPs.[39] BLG NPs may be ingested via the endocytosis of macrophages, as smaller and negatively charged particles were taken up more efficiently by macrophages than lager cationic liposomes.[40] The low cytotoxicity of P1 NPs may be attributed to the negative surface charge (−35 mV) and particles size ranged mainly between 100–200 nm, as was found in the cytotoxicity assessment of heparin NPs in NR8383 macrophages[41] and as that of branched polyethylenimine NPs in Hela and Hep-G2 cells.[42] As was shown in silver NPs[43] and organic monolayer-coated silicon NPs,[44] the size-/surface charge-dependent generation of intracellular reactive oxygen species may be the acting mechanism of BLG NPs' cytotoxicity. The selective cellular activities of BLG NPs and MXSGT NPs[15] may imply an advantage of these 'natural occurred' nanoassemblies, and a potential of developing a smart protein nanovehicle for target delivery of anti-cancerogenic drug accordingly.

Furthermore, swelling/shrinking behavior of NPs in simultaneous response to temperature and pH characterized them as intelligent polymers, which are of particular interests in the search of drug vehicle targeting life-threatening diseases, i.e. cancer. The NPs maintained the smallest particles size at boiling temperature or native pH of BLG decoction (nearly pH 5). Change of either temperature or pH resulted in the swelling behavior of NPs in BLG soups, which may work as a switch for controlled release of phytochemicals carried by these "decoction-derived" NPs.[15]

Protein glycation may be essential for the formation of BLG NPs. Despite the high content of non-glycated proteins in the fresh roots, the total protein content in the soluble and colloidal portion of the fresh roots decoction was much lower than its sun-dried counterparts (BLG decoction). The SEC chromatogram of fresh roots decoction showed poor absorption at UV280 nm and weak light scattering intensity, implying the relevance between protein glycation occurred during the sun-dried process and the formation of

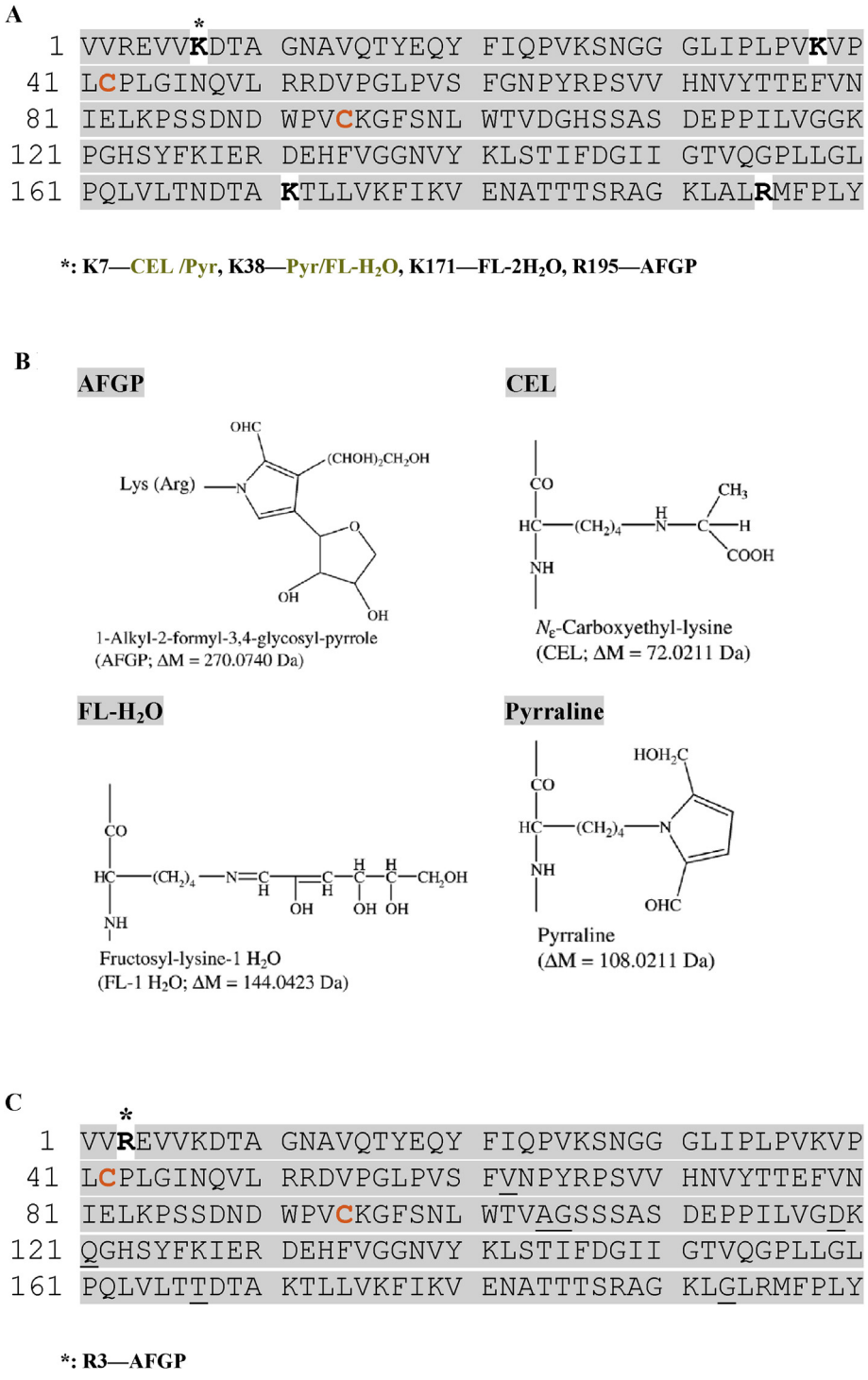

Fig. 9. (A) Full amino acid sequence and glycation adducts of BLGP1. (B) Four types of glycation adducts found in BLGPs. (C) Full amino acid sequence and glycation adducts of BLGP2.

protein-based NPs in BLG decoction. As is well-documented, non-enzymatic glycation endows the glycated proteins with thermal stability and the colloidal aggregates forming ability, of which the native proteins may not be capable.[27]

To better understand the chemical and primary structural nature of the self-assembly BLG NPs, cDNA cloning and glycation sites analysis were carried out on the BLGP proteins. The primary structure alignments revealed very high homology in these two BLGP proteins, which just represent allelic variants of the same gene. These NPs assembled by single-gene-coded proteins revealed a surprisingly simple model for studying the bioactive particulates derived from multiple composition systems as complex as an herbal decoction.

The full-length protein sequences suggest the possible glycation sites: 7 arginine residues, 12 lysine residues and 2 cysteine residues in both BLGP proteins. The theoretical molecular weights of native proteins are a few hundred Dalton less than those of experimental data, which is in agree with the fact that glycation increase protein

molecular weight. Indicated by the accurate mass difference between hydrolyzed peptides identified in the glycated and non-glycated BLGP proteins, all glycation adducts are early glycation products derived from lysine and arginine. Neither cysteine residue modification nor advanced glycation products was detected. Therefore, the glycated BLGP proteins may be used as a simplified model to study the self-assembly mechanism of glycated proteins derived from heat processed food. Knowing chemical and physical characteristics of the protein, the overall structural information upon its conformation and nano-assemblies can be studied with a range of analytical methods including circular dichroism spectroscopy, Fourier transform infrared spectroscopy and fluorescence spectra.[45]

5. Conclusion

In summary, protein-based NPs (mean diameter 120 nm) were isolated and characterized from BLG decoction. These naturally occurred NPs showed potential as nutrient/drug carriers with either cyto-selective bioactivities or temperature- and pH-sensitive reversible conformations, providing a novel prototype for herb-based nanomedicine development. The SEC isolated BLG NPs promoted the growth of normal cells but suppressed that of cancerogenic cells and macrophages, which was possibly attributed to the size and surface charge dependent uptake of NPs in different types of cells. The glycated BLGP proteins with self-assembly capacity are of particular relevance to the formation of nanoparticles. The sequence mapping and glycation site analysis of BLGP proteins have revealed some chemical changes relevant to the NPs self-assembly, while assembly mechanism is not yet elucidated. Besides, further work is warranted to investigate the stability, loading/releasing and bioavailability of nanoparticle self-assembled with pure BLGP proteins. After all, the future value of this study lies in developing novel, intelligent, heat-stable and safe nano-materials for delivery of bioactive compounds, apart from disclosing the function and safety impacts that nanoparticles may possess in herbal decoctions. “From nature to novel”, this would be most important strength that modern science could inherit from traditional knowledge.

Conflict of interest

There is no conflict of interest.

Acknowledgments

This research was supported by the National Natural Science Foundation of China (Grant No. 31571803) and the Natural Science Foundation of Zhejiang Province of China (LY16C200001) and the Open Grant from Zhejiang Provincial Top Key Discipline of Food Science and Biotechnology (Grant No. JYTsp20141072).

References

1. Bensky D, Gamble A, Kaptchuk T. *Chinese Herbal Medicine: Materia Medica*. 1990th ed. Seattle: Eastland Press; 1993.
2. Huang K. *The Pharmacology of Chinese Herbs*. Boca Raton: CRC Press LLC; 1999.
3. Zhu Y. *Chinese Materia Medica*. Amsterdam: Overseas Publishers Association; 1998.
4. China Pharmacopeia Committee. *China Pharmacopeia*. 2005th ed. Beijing, China: Chemical Industry Press; 2005.
5. Ke Lijing, Wen Teng, Bradshaw Jeremy P, Zhou Jianwu, Rao Pingfan. Antiviral decoction of isatidis radix (板藍根 bǎn lán gēn) inhibited influenza virus adsorption on MDCK cells by cytoprotective activity. *J Tradit Complement Med*. 2012;2(1):47–51. http://www.jtcm.org/jtcm_n/portal_e6_page.php?button_num=e6&cnt_id=23. Accessed 16 January 2012.
6. Han J, Jiang X, Zhang L. Optimisation of extraction conditions for polysaccharides from the roots of *Isatis tinctoria* L. by response surface methodology and their in vitro free radicals scavenging activities and effects on IL-4 and IFN-γ mRNA expression in chicken lymphocytes. *Carbohydr Polym*. 2011;86(3):1320–1326. http://dx.doi.org/10.1016/j.carbpol.2011.06.036.
7. Xiang L, Wang H, Lu H, et al. Analysis of amino acids in Banlangen during heating process. *Amino Acids Biotic Resour*. 2007;29(3):57–59.
8. Ghoshmoulick R, Bhattacharya J, Roy S, Basak S. Compensatory secondary structure alterations in protein glycation. *Sciences (New York)*. 2007;1774:233–242. http://dx.doi.org/10.1016/j.bbapap.2006.11.018.
9. Reddy GK, Stehno-bittel L, Enwemeka CS. Glycation-induced matrix stability in the rabbit Achilles tendon. *Arch Biochem Biophys*. 2002;399(2):174–180. http://dx.doi.org/10.1006/abbi.2001.2747.
10. Zhuang Y, Yan J, Zhu W, Chen L, Liang D, Xu X. Can the aggregation be a new approach for understanding the mechanism of Traditional Chinese Medicine? *J Ethnopharmacol*. 2008;117(2):378–384. http://dx.doi.org/10.1016/j.jep.2008.02.017.
11. Zhang J-M, Liao W, He Y, He Y, Yan D, Fu C-M. Study on intestinal absorption and pharmacokinetic characterization of diester diterpenoid alkaloids in precipitation derived from fuzi-gancao herb-pair decoction for its potential interaction mechanism investigation. *J Ethnopharmacol*. 2013;147(1):128–135. http://dx.doi.org/10.1016/j.jep.2013.02.019.
12. Wang L, Zhou G, Liu P, et al. Dissection of mechanisms of Chinese medicinal formula Realgar-*Indigo* naturalis as an effective treatment for promyelocytic leukemia. *Proc. Natl. Acad. Sci.* 2008;105(12):4826–4831. http://www.pnas.orgcgidoi10.1073pnas.0712365105.
13. Flower A, Lewith G, Little P. Combining rigour with relevance: a novel methodology for testing Chinese herbal medicine. *J Ethnopharmacol*. 2011;134(2):373–378. http://dx.doi.org/10.1016/j.jep.2010.12.025.
14. Ma XH, Zheng CJ, Han LY, et al. Synergistic therapeutic actions of herbal ingredients and their mechanisms from molecular interaction and network perspectives. *Drug Discov Today*. 2009;14(11–12):579–588. http://dx.doi.org/10.1016/j.drudis.2009.03.012.
15. Zhou J, Gao G, Chu Q, Wang H, Rao P, Ke L. Chromatographic isolation of nanoparticles from Ma-Xing-Shi-Gan-Tang decoction and their characterization. *J Ethnopharmacol*. 2014;151(3):1116–1123. http://dx.doi.org/10.1016/j.jep.2013.12.029.
16. Hu J, Wu Z, Yan J, Pang W, Liang D, Xu X. A promising approach for understanding the mechanism of Traditional Chinese. *J Ethnopharmacol*. 2009. http://dx.doi.org/10.1016/j.jep.2009.03.007.
17. Wang G, Yang C, Zhang K, Hu J, Pang W. Molecular clusters size of *Puerariae thomsonii* radix aqueous decoction and relevance to oral absorption. *Molecules*. 2015;20(7):12376–12388. http://dx.doi.org/10.3390/molecules200712376.
18. Niseteo T, Komes D, Belščak-Cvitanović A, Horžić D, Budeč M. Bioactive composition and antioxidant potential of different commonly consumed coffee brews affected by their preparation technique and milk addition. *Food Chem*. 2012;134(4):1870–1877. http://dx.doi.org/10.1016/j.foodchem.2012.03.095.
19. Serafini M, Bugianesi R, Maiani G, Valtuena S, De Santis S, Crozier A. Plasma antioxidants from chocolate. *Nature*. 2003;424(6952):1013. http://dx.doi.org/10.1038/4241013a.
20. Matalanis A, Jones OG, McClements DJ. Structured biopolymer-based delivery systems for encapsulation, protection, and release of lipophilic compounds. *Food Hydrocoll*. 2011;25(8):1865–1880. http://dx.doi.org/10.1016/j.foodhyd.2011.04.014.
21. Lai LF, Guo HX. Preparation of new 5-fluorouracil-loaded zein nanoparticles for liver targeting. *Int J Pharm*. 2011;404(1–2):317–323. http://dx.doi.org/10.1016/j.ijpharm.2010.11.025.
22. San Biagio PL, Martorana V, Emanuele A, et al. Interacting processes in protein coagulation. *Proteins*. 1999;37(1):116–120. http://www.ncbi.nlm.nih.gov/pubmed/10451555. Accessed 16 December 2014.
23. Rondeau P, Navarra G, Cacciabaudo F, Leone M, Bourdon E, Militello V. Thermal aggregation of glycated bovine serum albumin. *Biochim Biophys Acta*. 2010;1804(4):789–798. http://dx.doi.org/10.1016/j.bbapap.2009.12.003.
24. Militello V, Casarino C, Emanuele A, Giostra A, Pullara F, Leone M. Aggregation kinetics of bovine serum albumin studied by FTIR spectroscopy and light scattering. *Biophys Chem*. 2004;107(2):175–187. http://dx.doi.org/10.1016/j.bpc.2003.09.004.
25. Thorpe SR, Baynes JW. Maillard reaction products in tissue proteins: new products and new perspective. *Amino Acids*. 2003:275–281. http://dx.doi.org/10.1007/s00726-003-0017-9.
26. Liu J, Ru Q, Ding Y. Glycation a promising method for food protein modification: physicochemical properties and structure, a review. *Food Res Int*. 2012;49(1):170–183. http://dx.doi.org/10.1016/j.foodres.2012.07.034.
27. Wooster TJ, Augustin MA. Beta-lactoglobulin-dextran Maillard conjugates: their effect on interfacial thickness and emulsion stability. *J Colloid Interface Sci*. 2006;303(2):564–572. http://dx.doi.org/10.1016/j.jcis.2006.07.081.
28. Laemmli UK. Cleavage of structural proteins during the assembly of the head of bacteriophage T4. *Nature*. 1970;227(5259):680–685. http://www.ncbi.nlm.nih.gov/pubmed/5432063. Accessed 26 July 2010.
29. Wa C, Cerny RL, Clarke WA, Hage DS. Characterization of glycation adducts on human serum albumin by matrix-assisted laser desorption/ionization time-of-flight mass spectrometry. *Clin Chim Acta*. 2007;385(1–2):48–60. http://dx.doi.org/10.1016/j.cca.2007.06.011.
30. Nguyen S, Hisiger S, Jolicoeur M, Winnik FM, Buschmann MD. Fractionation and characterization of chitosan by analytical SEC and 1H NMR after semi-preparative SEC. *Carbohydr Polym*. 2009;75(4):636–645. http://dx.doi.org/10.1016/j.carbpol.2008.09.002.

31. Yan J-K, Cai P-F, Cao X-Q, et al. Green synthesis of silver nanoparticles using 4-acetamido-TEMPO-oxidized curdlan. *Carbohydr Polym*. 2013;97(2):391–397. http://dx.doi.org/10.1016/j.carbpol.2013.05.049.
32. Kong N, Jiang T, Zhou Z, Fu J. Cytotoxicity of polymerized resin cements on human dental pulp cells in vitro. *Dent Mater*. 2009;25(11):1371–1375. http://dx.doi.org/10.1016/j.dental.2009.06.008.
33. Lanone S, Rogerieux F, Geys J, et al. Comparative toxicity of 24 manufactured nanoparticles in human alveolar epithelial and macrophage cell lines. *Part Fibre Toxicol*. 2009;6(1):14. http://dx.doi.org/10.1186/1743-8977-6-14.
34. Mahler H-C, Friess W, Grauschopf U, Kiese S. Protein aggregation: pathways, induction factors and analysis. *J Pharm Sci*. 2009;98(9):2909–2934. http://dx.doi.org/10.1002/jps.21566.
35. Ke L, Zhou J, Lu W, Gao G, Rao P. The power of soups: super-hero or team-work? *Trends Food Sci Technol*. 2011;22(9):492–497. http://dx.doi.org/10.1016/j.tifs.2011.06.004.
36. Wang W-X, Pelah D, Alergand T, Shoseyov O, Altman A. Characterization of SP1, a stress-responsive, boiling-soluble, homo-oligomeric protein from aspen. *Plant Physiol*. 2002;130(2):865–875. http://dx.doi.org/10.1104/pp.002436.
37. Medalsy I, Dgany O, Sowwan M, et al. SP1 protein-based nanostructures and arrays. *Nano Lett*. 2008;8(2):473–477. http://dx.doi.org/10.1021/nl072455t.
38. Oberdörster G, Oberdörster E, Oberdörster J. Nanotoxicology: an emerging discipline evolving from studies of ultrafine particles. *Environ Health Perspect*. 2005;113(7):823–839. http://dx.doi.org/10.1289/ehp.7339.
39. Fröhlich E. The role of surface charge in cellular uptake and cytotoxicity of medical nanoparticles. *Int J Nanomed*. 2012;7:5577–5591. http://dx.doi.org/10.2147/IJN.S36111.
40. Epstein-Barash H, Gutman D, Markovsky E, et al. Physicochemical parameters affecting liposomal bisphosphonates bioactivity for restenosis therapy: internalization, cell inhibition, activation of cytokines and complement, and mechanism of cell death. *J Control Release*. 2010;146(2):182–195. http://dx.doi.org/10.1016/j.jconrel.2010.03.011.
41. Eidi H, Joubert O, Attik G, et al. Cytotoxicity assessment of heparin nanoparticles in NR8383 macrophages. *Int J Pharm*. 2010;396(1–2):156–165. http://dx.doi.org/10.1016/j.ijpharm.2010.06.006.
42. Pathak A, Kumar P, Chuttani K, et al. Gene expression, biodistribution, and pharmacoscintigraphic evaluation of chondroitin sulfate-PEI nanoconstructs mediated tumor gene therapy. *ACS Nano*. 2009;3(6):1493–1505. http://dx.doi.org/10.1021/nn900044f.
43. Carlson C, Hussain SM, Schrand AM, et al. Unique cellular interaction of silver nanoparticles: size-dependent generation of reactive oxygen species. *J Phys Chem B*. 2008;112(43):13608–13619. http://dx.doi.org/10.1021/jp712087m.
44. Bhattacharjee S, de Haan LHJ, Evers NM, et al. Role of surface charge and oxidative stress in cytotoxicity of organic monolayer-coated silicon nanoparticles towards macrophage NR8383 cells. *Part Fibre Toxicol*. 2010;7(1):25. http://dx.doi.org/10.1186/1743-8977-7-25.
45. Huang X, Tu Z, Wang H, et al. Probing the conformational changes of ovalbumin after glycation using HDX-MS. *Food Chem*. 2015;166:62–67. http://dx.doi.org/10.1016/j.foodchem.2014.05.155.